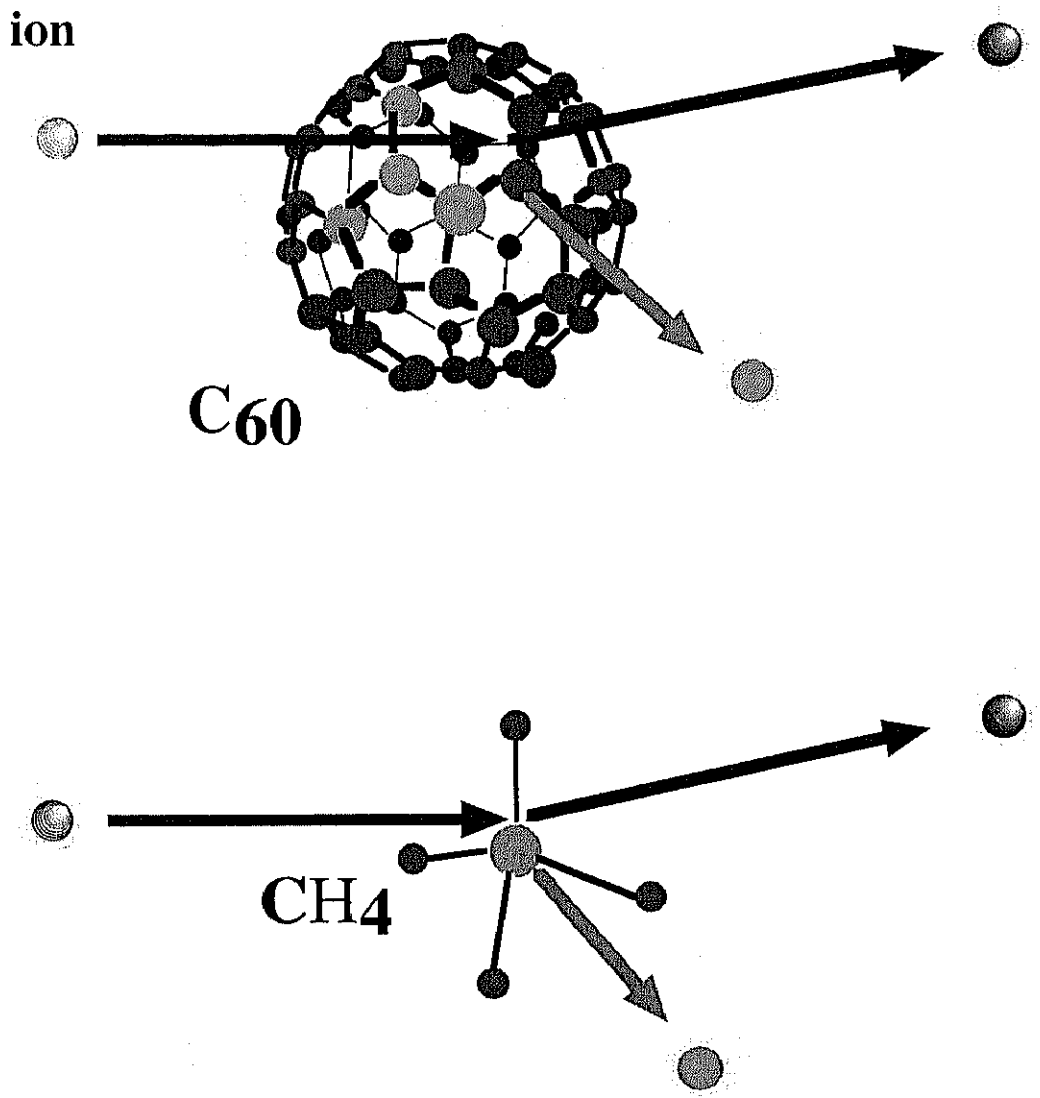

Figure 1: A schematic drawing of present experiments: C_{60} and CH_4 are gas target of mono molecule in space. Several kinds of noble gas ion are injected to it and recoiled carbon atoms are detected for each large angles. Angular distributions were compared with each target.

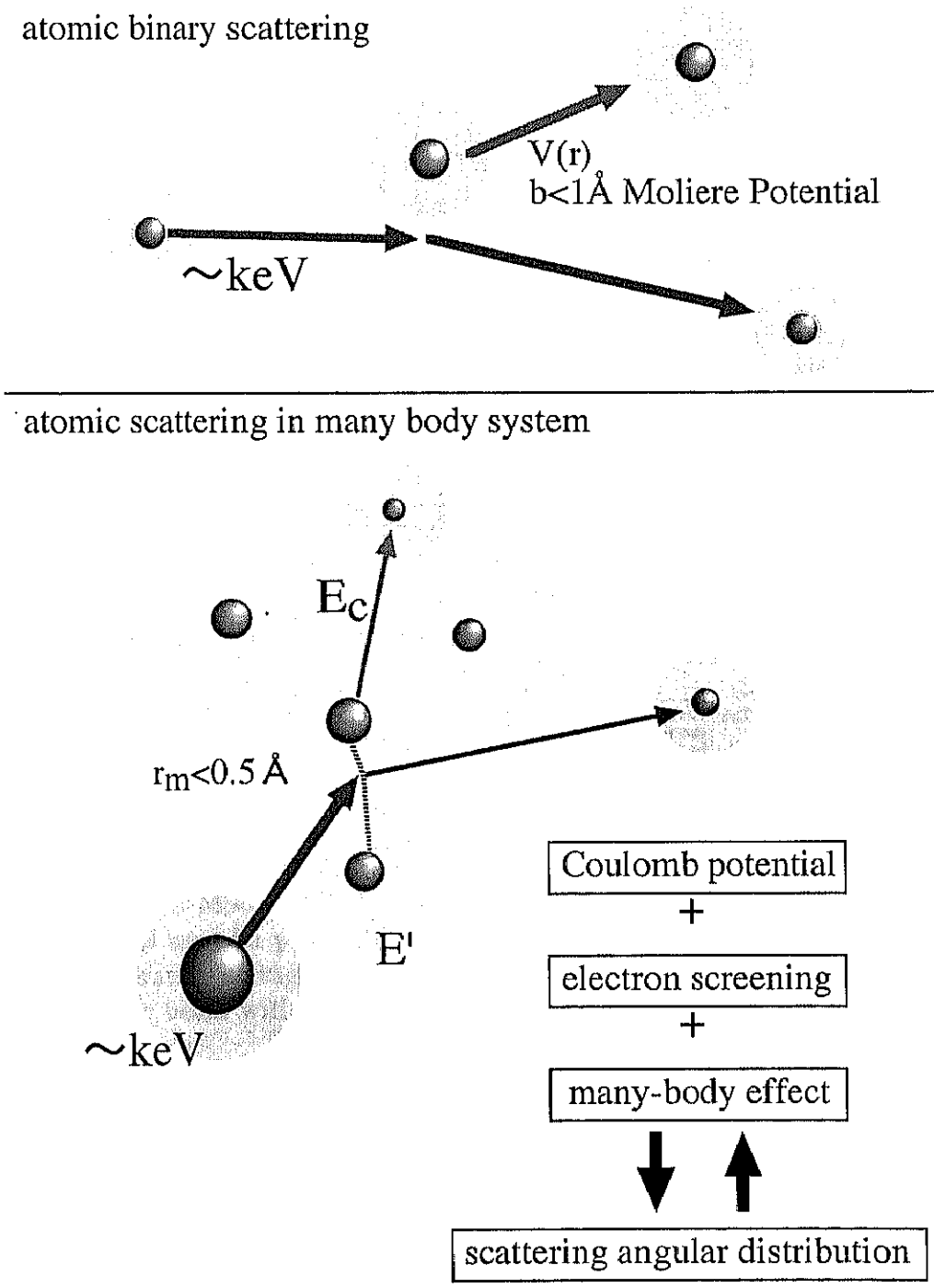

Figure 2: A schematic drawing of the aim of measuring the angular distributions: The scattering angular distributions include true information of interatomic potential concerning with scattering mechanism

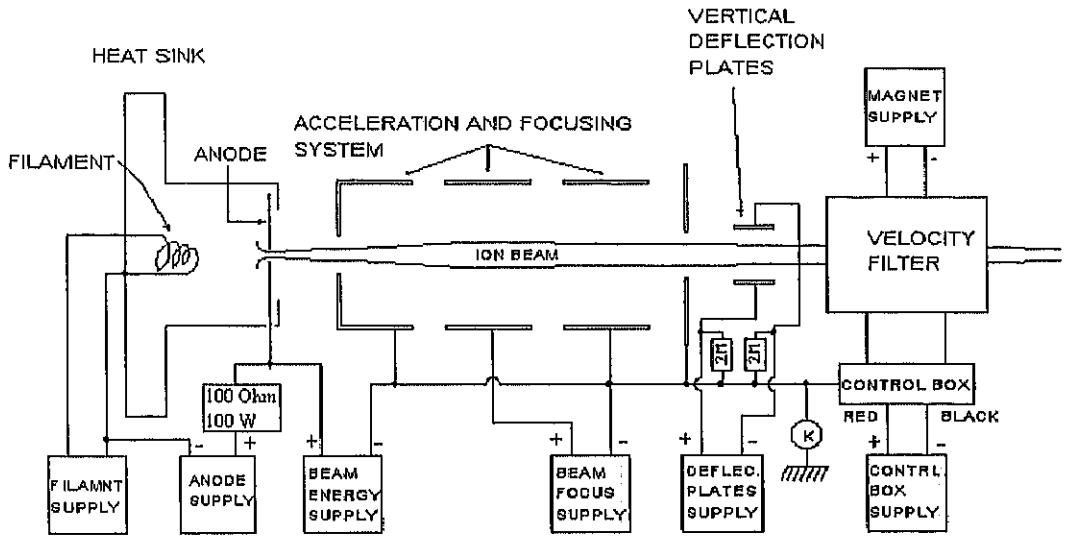

Figure 3: A schematic diagram of the Colutron ion source: Colutron Ion Source System Model G-2-D is produced by Colutron Research Co.. This ion source is used for production any ion beams from gas to material source with acceleration voltage up to 10kV as μA direct current. The velocity filter selects a ion beam with state of m/q.

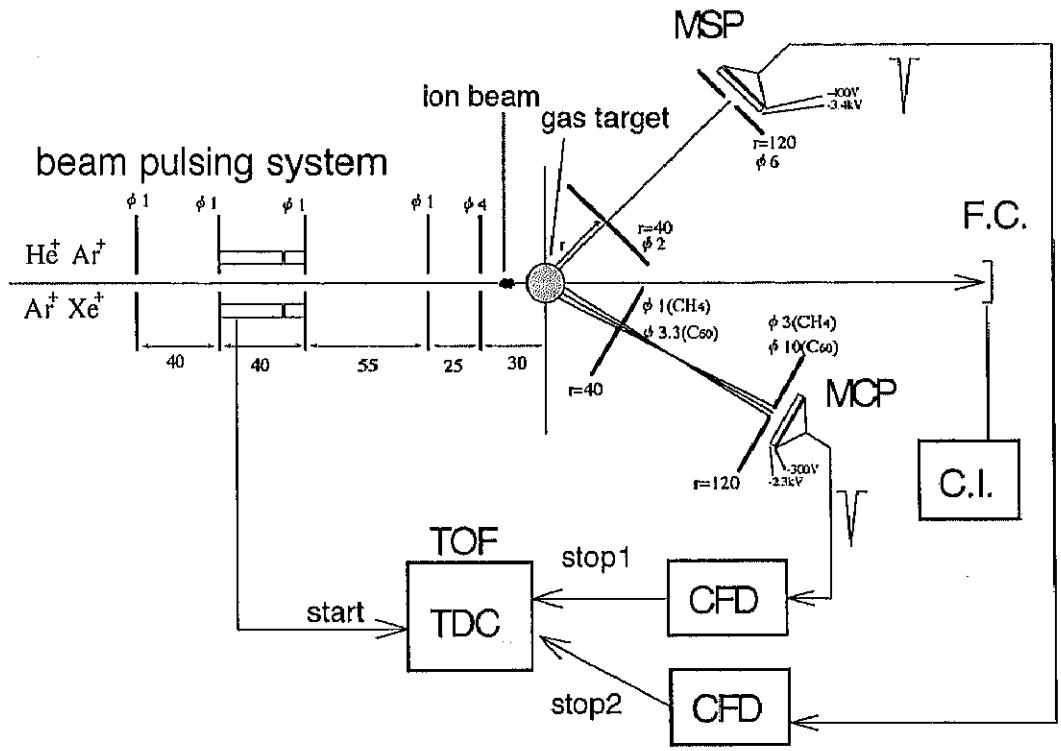

Figure 4: A schematic diagram of experimental setup for angular distribution measurement of atomic scattering: Incident beam was pulsed in front of collision point. All scattered atoms are identified by time of flight measurement and kinematic calculations suggest elastic scattering.

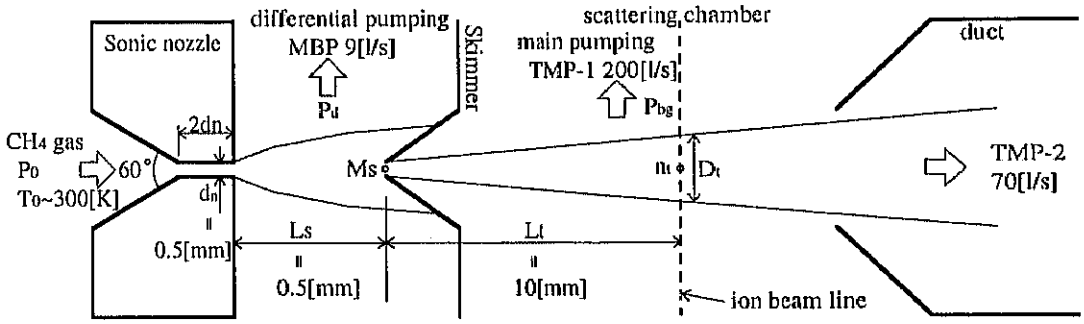

Figure 5: A schematic diagram of the supersonic molecular beam source: This system make possible a gas target with any gas phase reagent in high number of density, in spite of full open to all over the scattering angles.

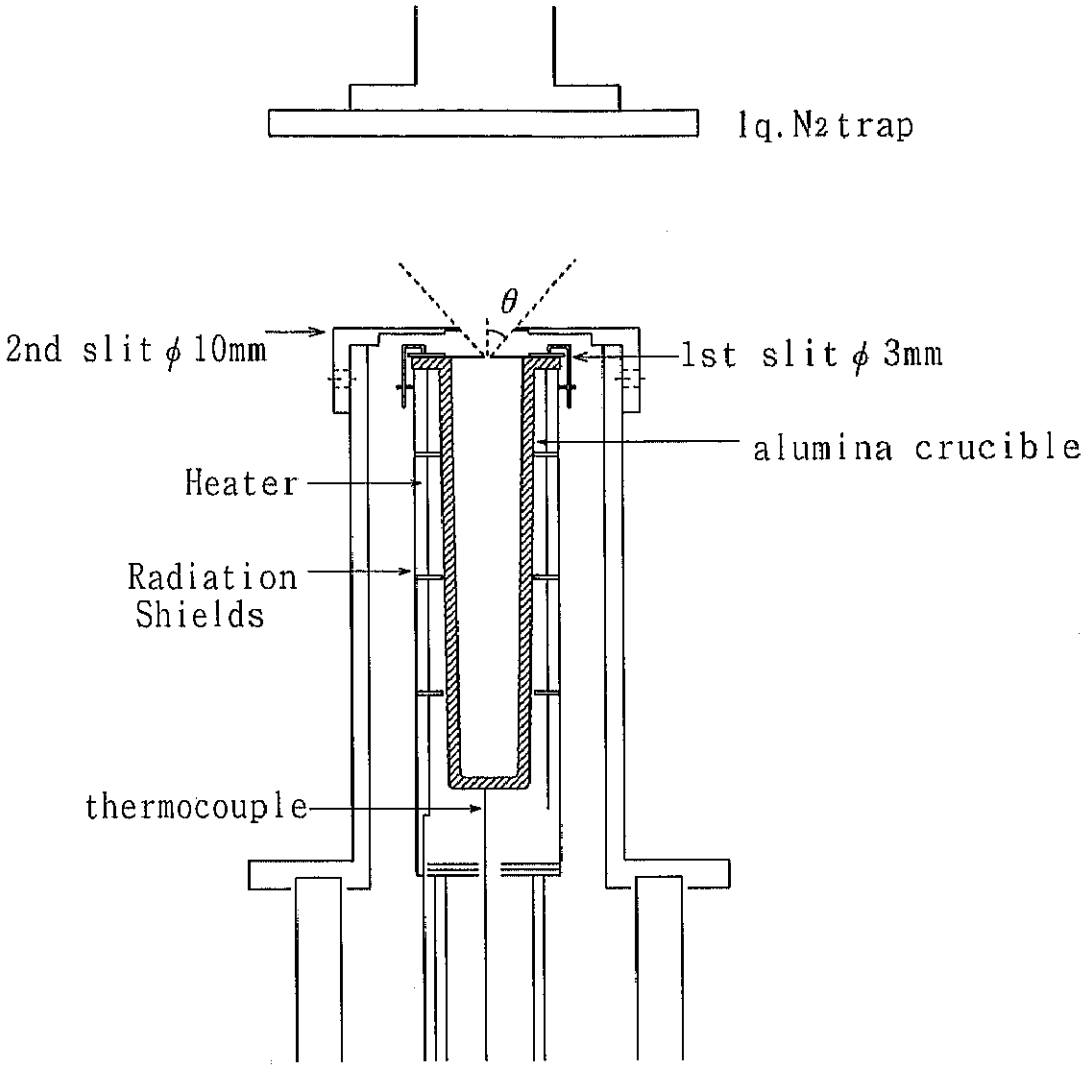

Figure 6: A schematic diagram of the effusive molecular beam source: This system make possible a gas target using any solid state reagent which has some vapor pressure by heating to several hundred degrees like C_{60}. It is also full open to all over the scattering angles.

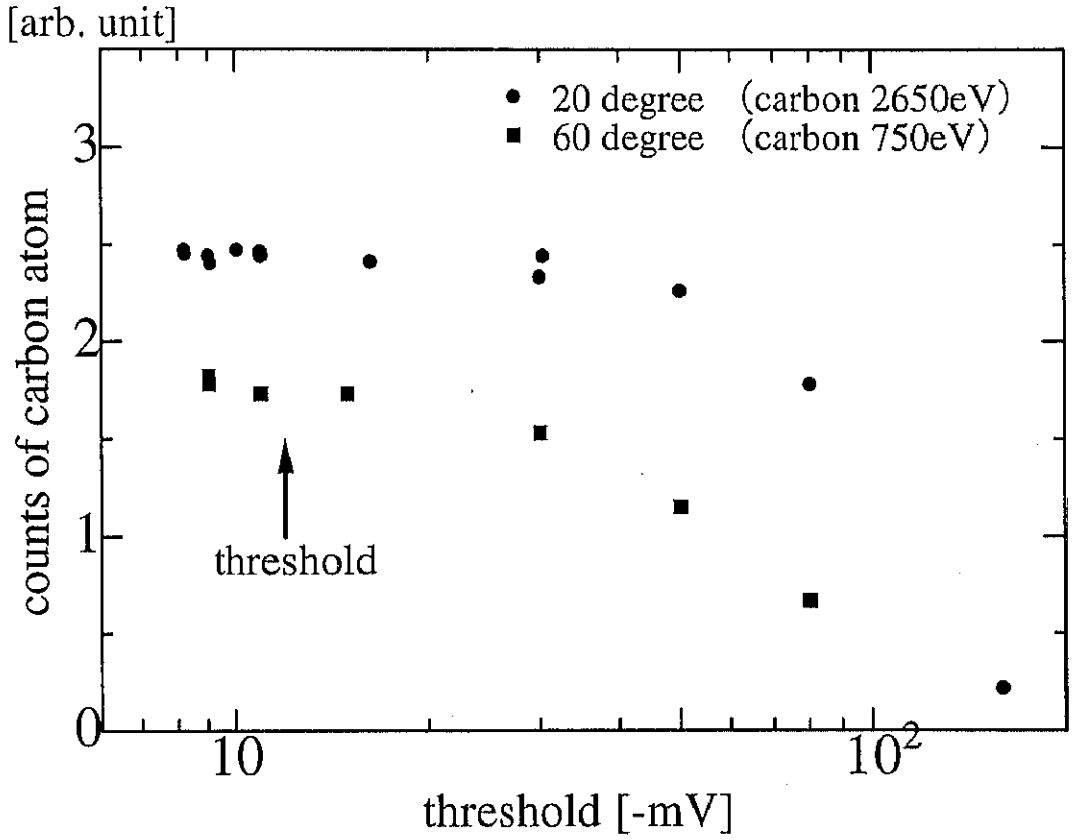

Figure 7: The counting rate of the scattered carbon atoms as changing the threshold level of the discriminator: The pulse height distribution of the signal from MCP anode is relatively broad in general way. The saturation of particle counts by MCP was checked on experimentally in this graph. This results indicate the correctness of pulse counting electrical circuit.

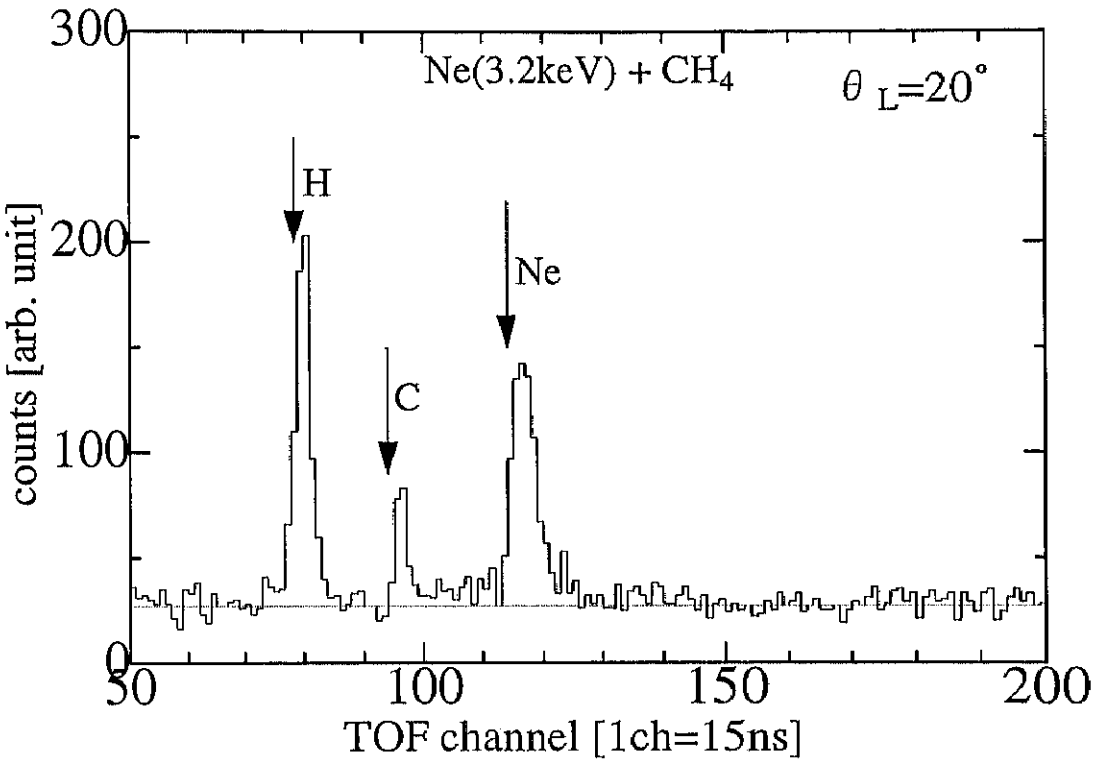

Figure 8: The typical TOF spectrum of scattered particles produced by collision Ne^+ on CH_4 *target* target at 3.2keV to 20° in laboratory coordinate: The arrows indicate the result of elastic scattering calculation between each pair of projectile and target atom. The kinds of recoiled atom are well identified. A noise level is indicated in dashed line.

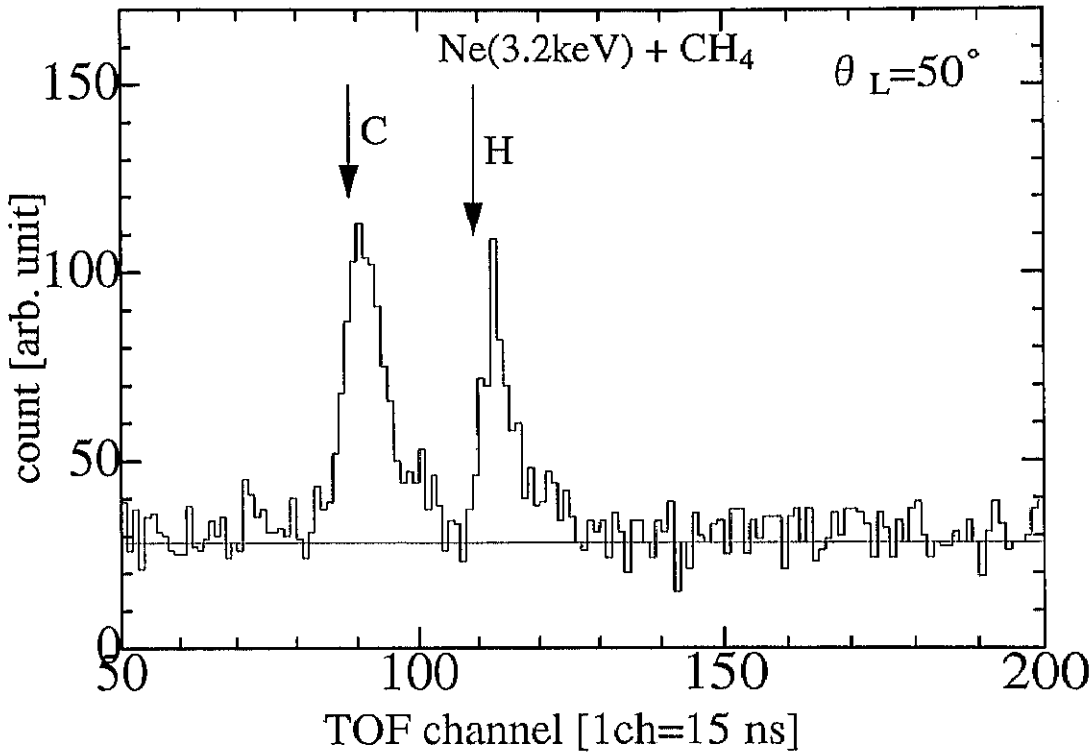

Figure 9: The TOF spectrum of scattered particles produced by collision Ne^+ on CH_4 *target* target at 3.2keV to 50° in laboratory coordinate: Ne atoms already vanish in such a large angles, because Ne has the limited scattering angular region calculated by kinematics of binary collision.

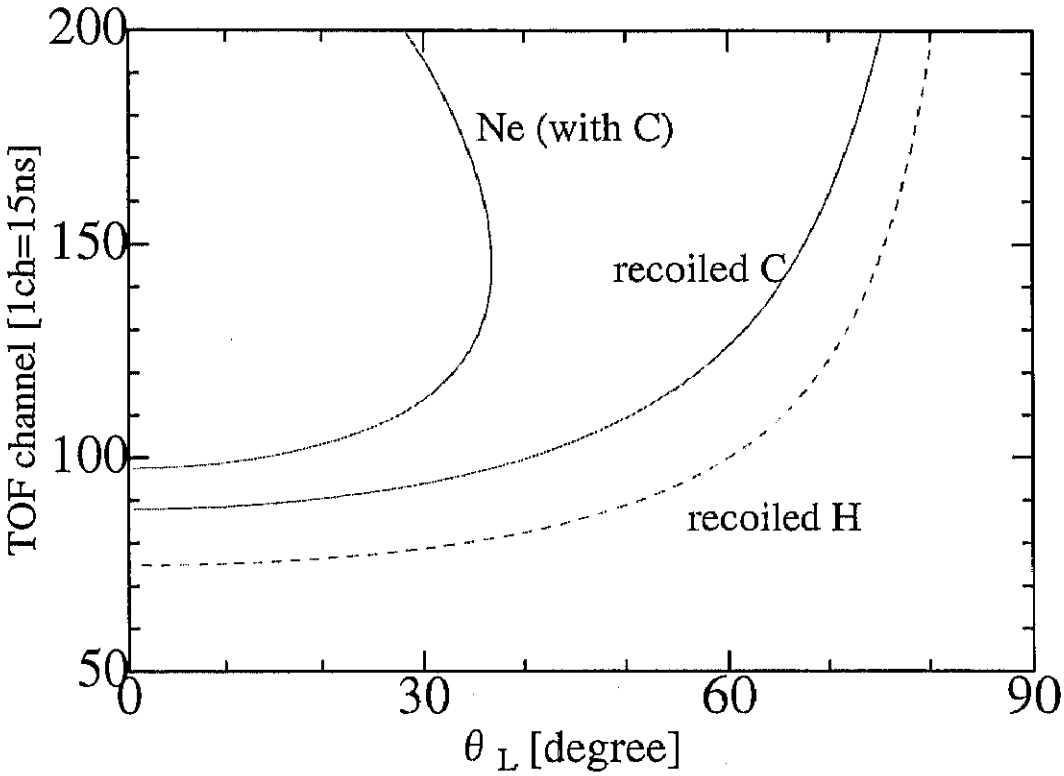

Figure 10: The results of TOF calculation as the function of scattering angle in laboratory coordinate based on the kinematical calculation of collision Ne with C and H target in elastic scattering:

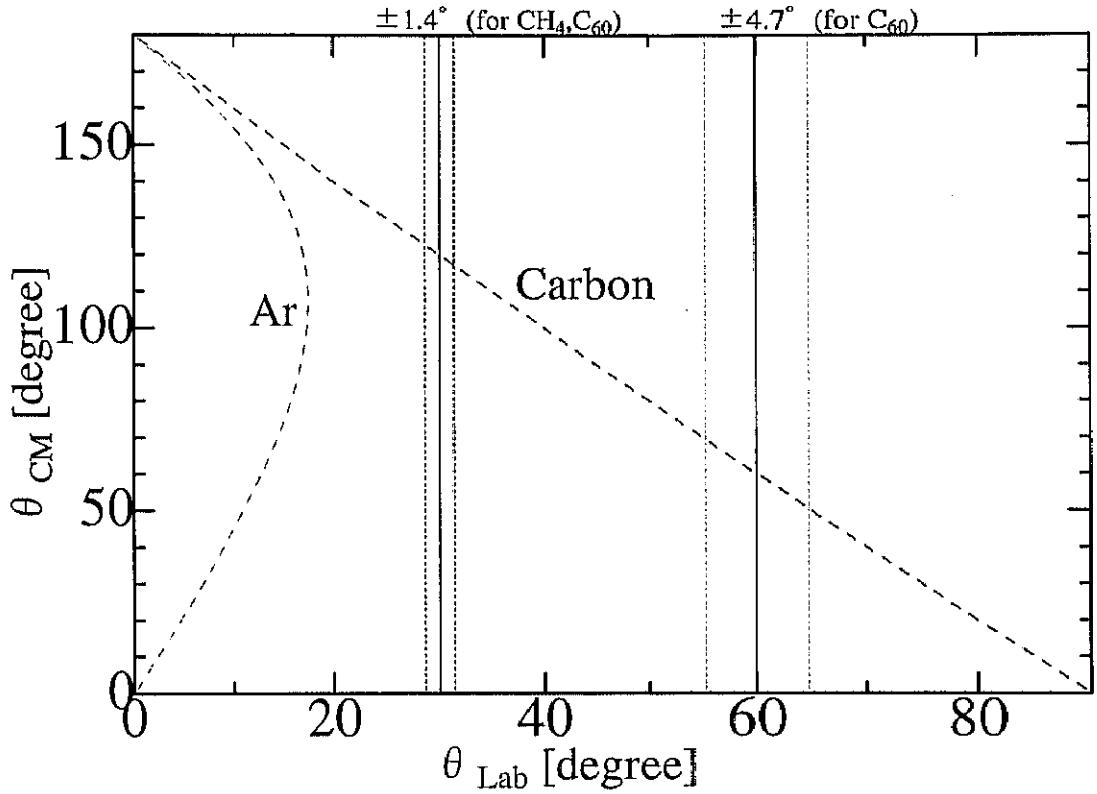

Figure 11: The collision angles in center of mass system as the function of the angle in laboratory system: When the incident atom is heavier than the target atom, the projectile scatters to the inside of the limited angles in laboratory system, but the angle of recoiled atom is fixed to $0° \sim 90°$ in any incident atoms. Therefore, detecting the recoiled carbon atoms is effective and advantageous methods for measuring angular distribution in wide angular region.

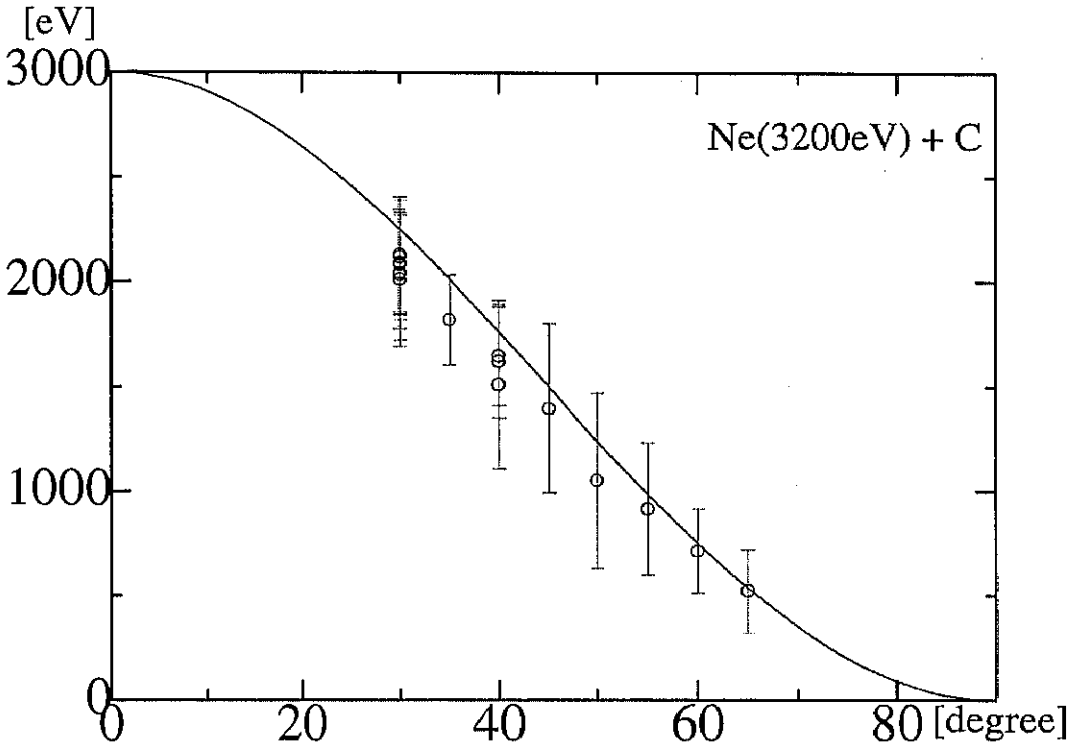

Figure 12: The measured recoil energy of a carbon atom with Ne^+ at 3.2 keV for C_{60} *target*: Error bars indicate FWHM of the each peak.

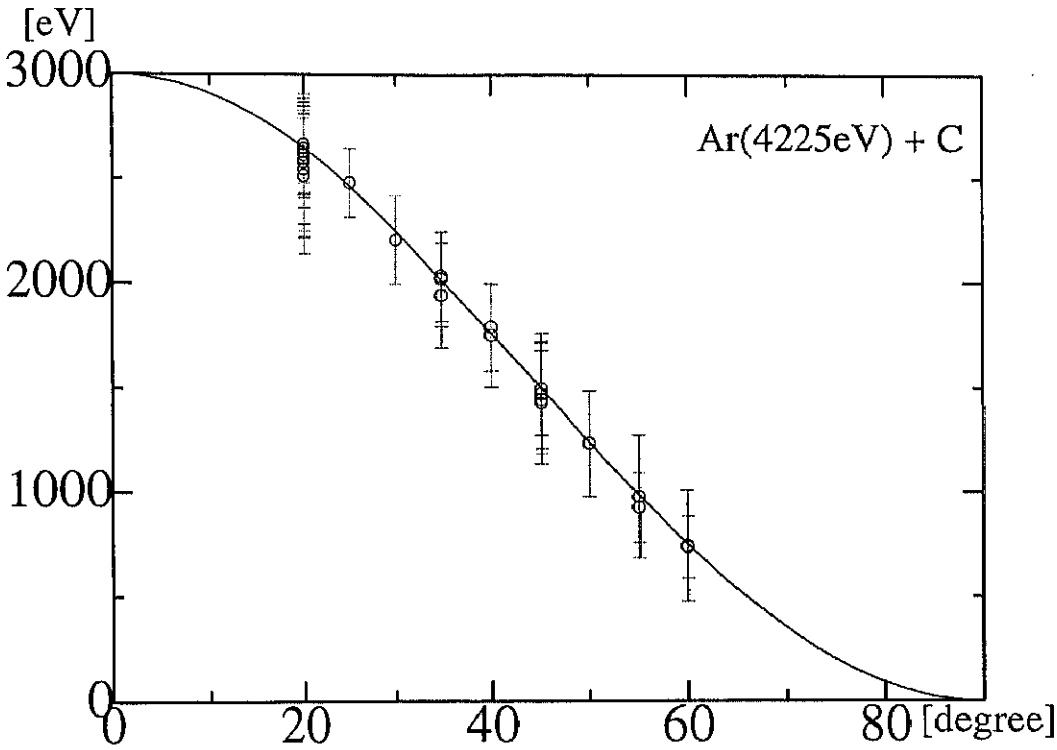

Figure 13: The measured recoil energy of a carbon atom with Ar^+ at 4225 eV for C_{60} *target*: Error bars indicate FWHM of the each peak.

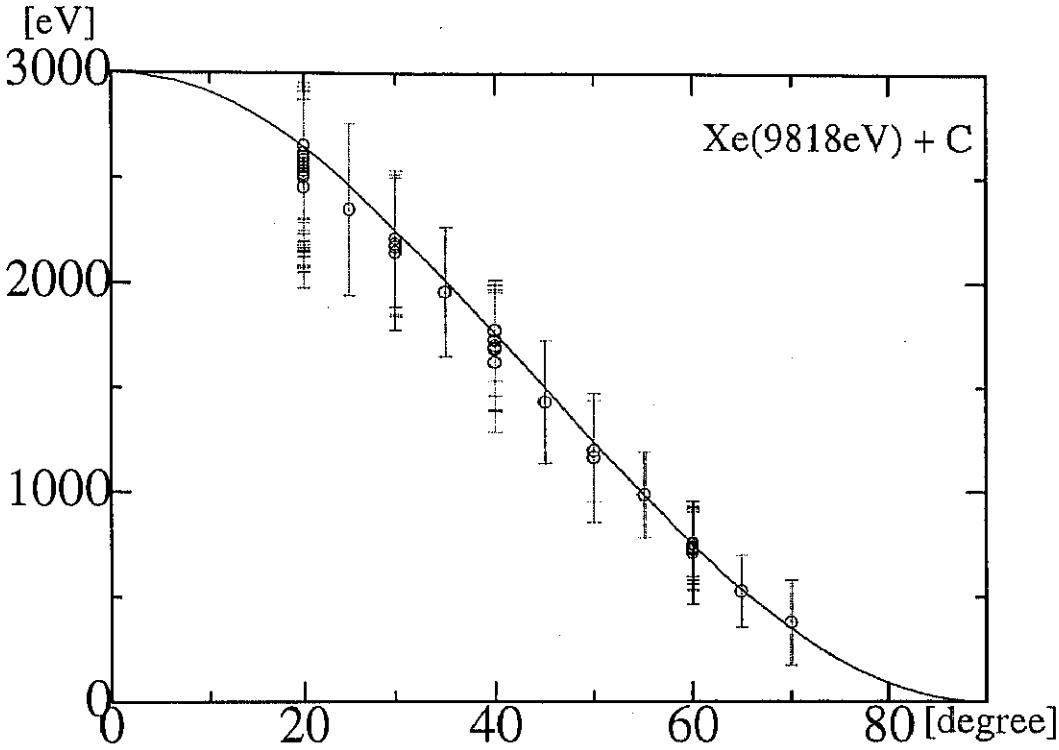

Figure 14: The measured recoil energy of a carbon atom with Xe^+ at 9818 eV for C_{60} *target*: Error bars indicate FWHM of the each peak.

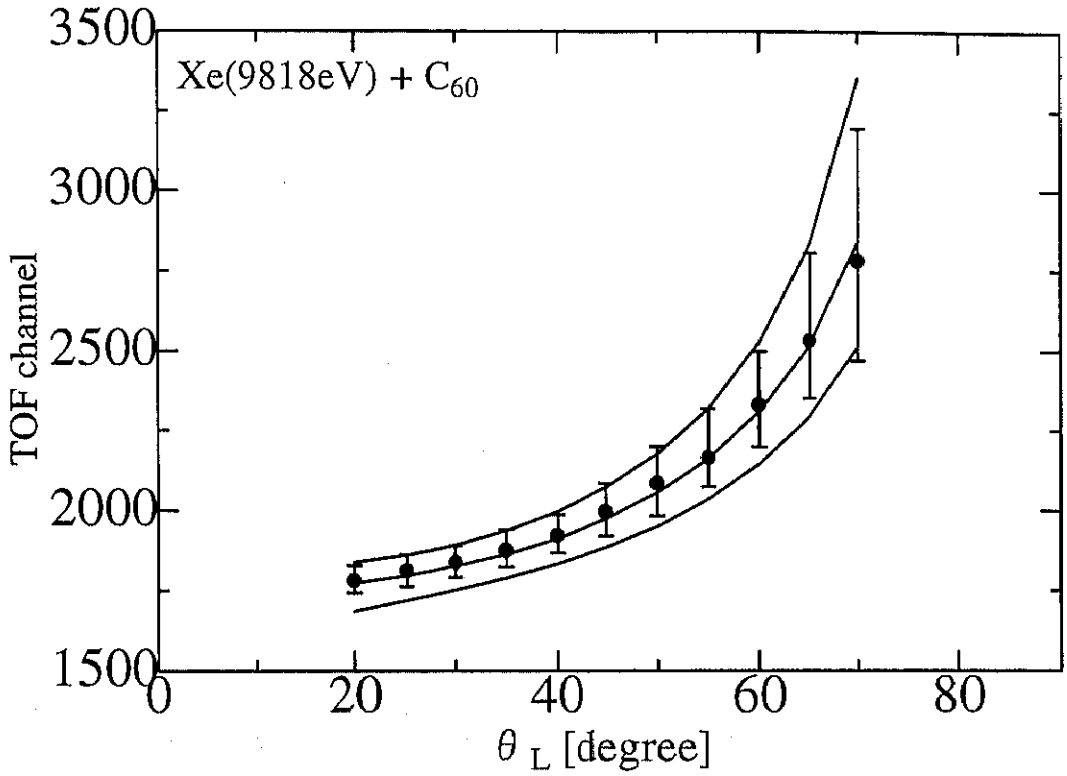

Figure 15: The measured TOF channel of carbon from collision Xe^+ (9818eV) on C_{60} *target* and theoretical calculations: The inside of the solid lines indicate the region of complete elastic scattering in present setup. The plots are TOF of the top of the peak and error bars are FWHM of it. In kinematical calculation, the quasi-binary atomic collisions should occur in C_{60}.

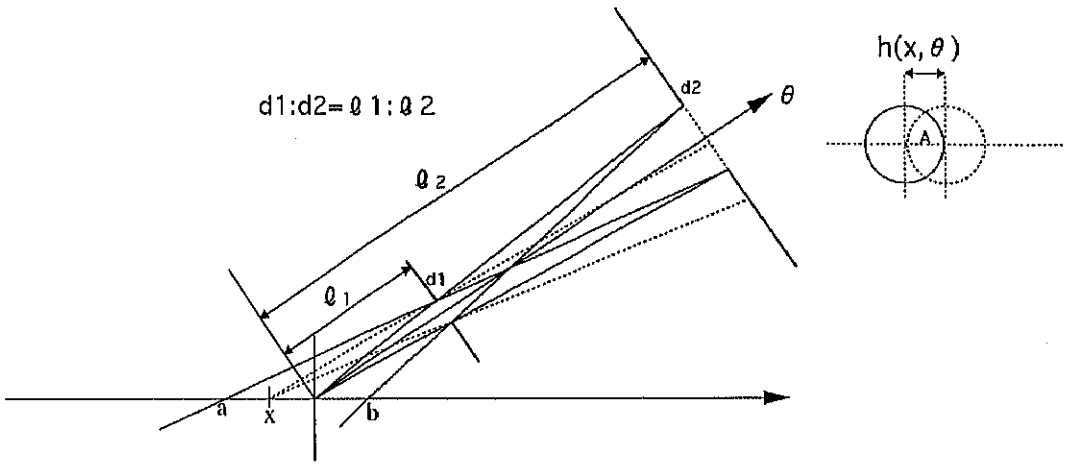

Figure 16: A schematic diagram of double slits in front of the entrance of detector for calculation effective solid angles: a and b are limit of view range of the detector. The dashed circle is the light spot from the first slit. A is a open area of the detector through the first and second slits from collision point, x.

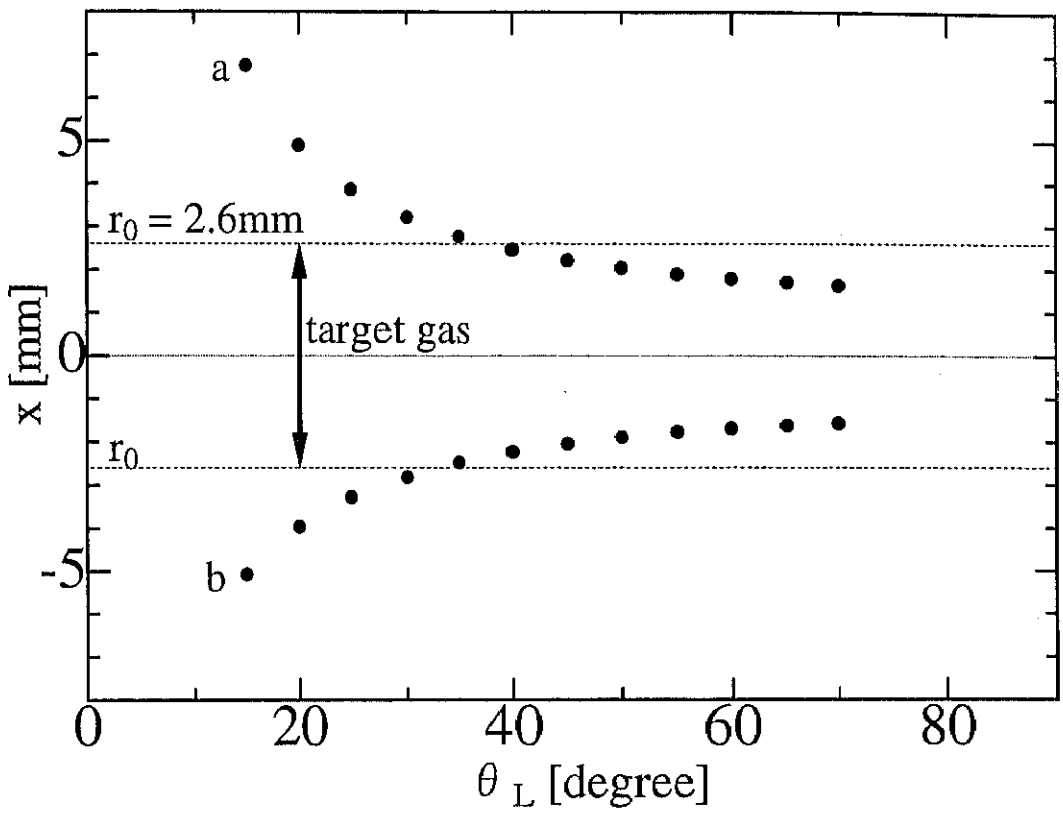

Figure 17: The peeping region of the detector for CH_4 experiments: The dashed lines indicate the area of the target spread radius, r_0. If a or b was larger than the radius, we only considered in target gas region for calculation of effective solid angles.

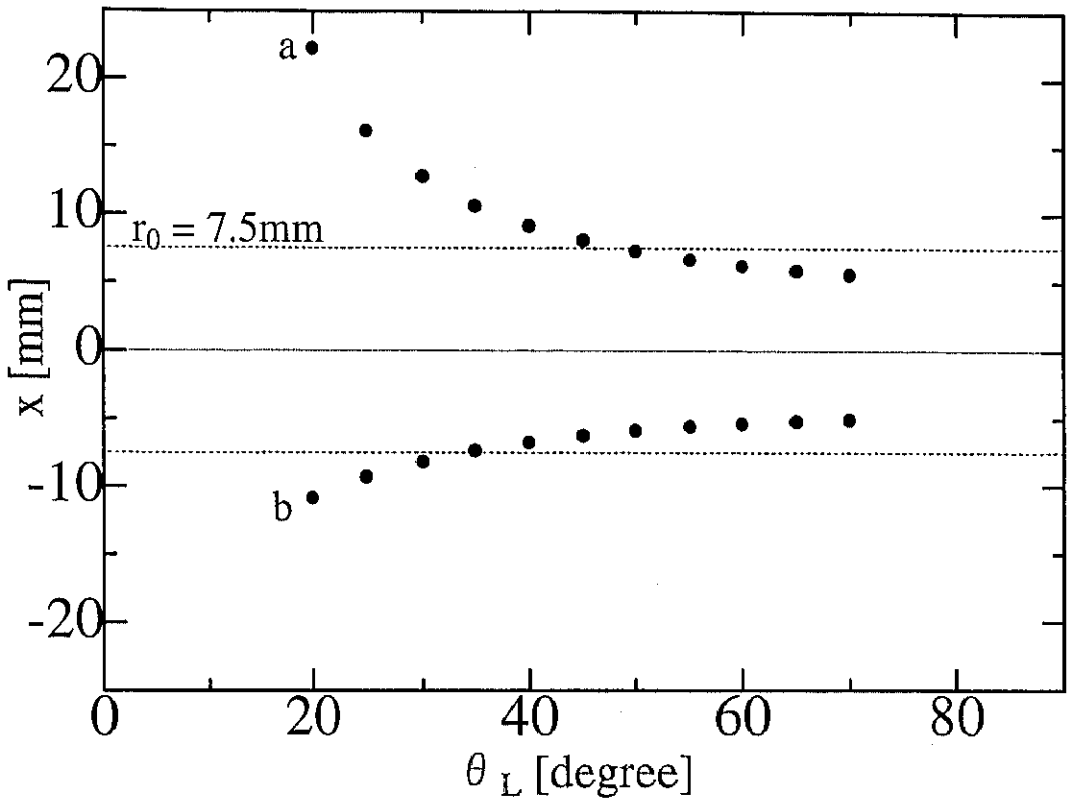

Figure 18: The peeping region of the detector for C_{60} experiments: The dashed lines indicate the area of the target spread radius, r_0. If a or b was larger than the radius, we only considered in target gas region for calculation of effective solid angles.

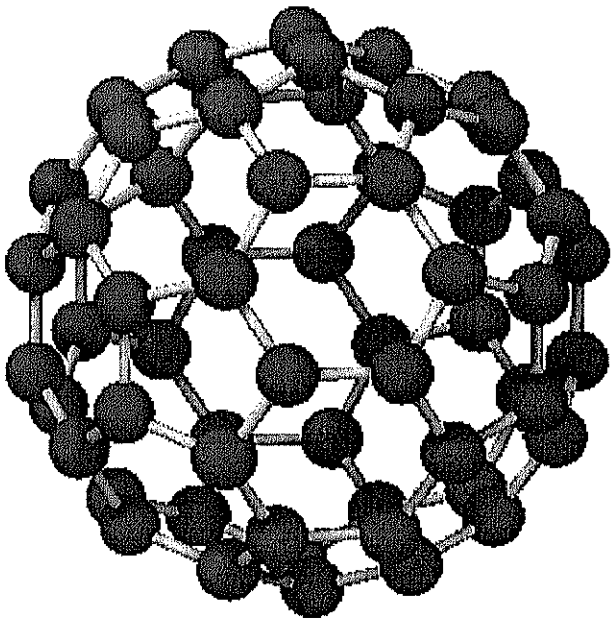

Figure 19: View of C_{60} molecule: The balls and bars indicate location of carbon atoms and σ-bonds of C_{60}, respectively.

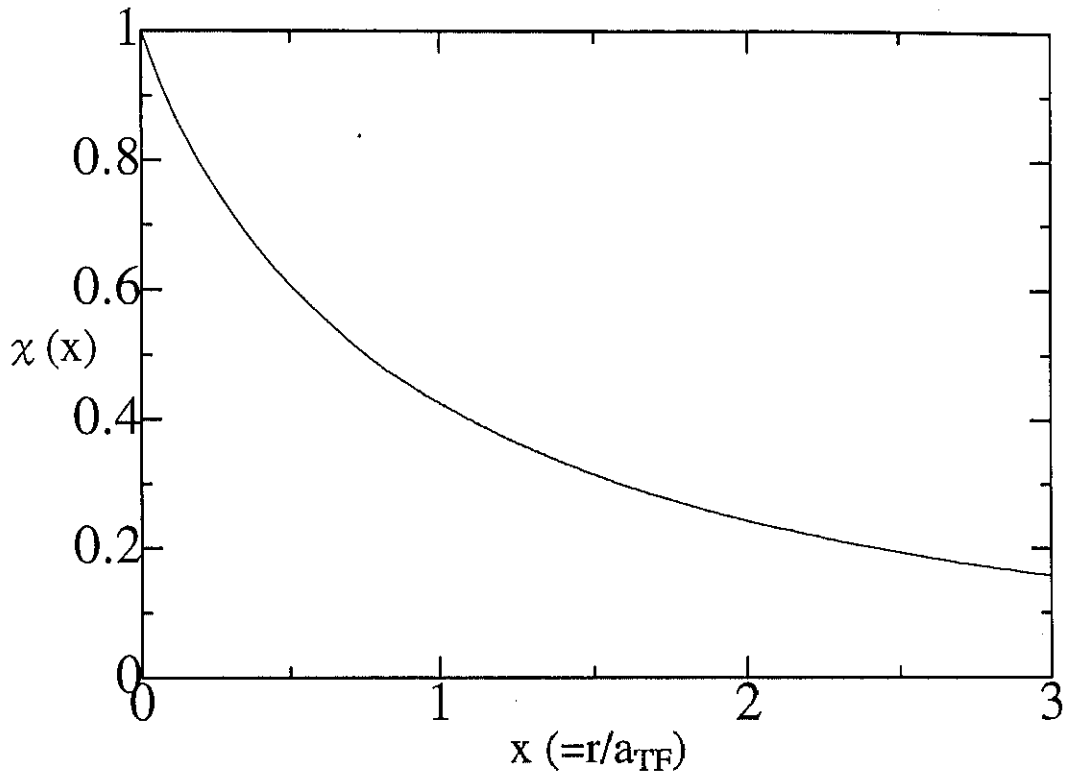

Figure 20: The curve of the approximate Thomas-Fermi screen function represented by Molière: χ value is the rate of suppressing for Coulomb force.